Soft Computing (2022) 26:13693–13708
https://doi.org/10.1007/s00500-022-07359-3

APPLICATION OF SOFT COMPUTING

Neuro-swarm computational heuristic for solving a nonlinear second-order coupled Emden–Fowler model

Zulqurnain Sabir[1] · Muhammad Asif Zahoor Raja[2] · Dumitru Baleanu[3,4] · Juan L. G. Guirao[5]

Accepted: 13 June 2022 / Published online: 25 July 2022

Abstract

The aim of the current study is to present the numerical solutions of a nonlinear second-order coupled Emden–Fowler equation by developing a neuro-swarming-based computing intelligent solver. The feedforward artificial neural networks (ANNs) are used for modelling, and optimization is carried out by the local/global search competences of particle swarm optimization (PSO) aided with capability of interior-point method (IPM), i.e., ANNs-PSO-IPM. In ANNs-PSO-IPM, a mean square error-based objective function is designed for nonlinear second-order coupled Emden–Fowler (EF) equations and then optimized using the combination of PSO-IPM. The inspiration to present the ANNs-PSO-IPM comes with a motive to depict a viable, detailed and consistent framework to tackle with such stiff/nonlinear second-order coupled EF system. The ANNs-PSO-IP scheme is verified for different examples of the second-order nonlinear-coupled EF equations. The achieved numerical outcomes for single as well as multiple trials of ANNs-PSO-IPM are incorporated to validate the reliability, viability and accuracy.

Keywords Coupled Emden–Fowler model · Interior-point algorithm · Neural networks · Numerical computing

Abbreviations

EF	Emden–Fowler
ANNs	Artificial neural networks
PSO	particle swarm optimization
IPM	interior-point method
RMSE	Root mean square error
VAF	Variance account for
SI	Semi interquartile
EVAF	Error in VAF
PSO-IPM	PSO aided with IPM
ANNs-PSO-IPM	ANNs optimized with PSO and IPM
MIN	Minimum
SD	Standard deviation

✉ Juan L. G. Guirao
juan.garcia@upct.es

Zulqurnain Sabir
zulqurnain_maths@hu.edu.pk

Muhammad Asif Zahoor Raja
rajamaz@yuntech.edu.tw

Dumitru Baleanu
dumitru@cankaya.edu.tr

1 Department of Mathematics and Statistics, Hazara University, Mansehra, Pakistan

2 Future Technology Research Center, National Yunlin University of Science and Technology, 123 University Road, Section 3, Douliou, Yunlin 64002, Taiwan, Republic of China

3 Department of Mathematics, Turkey d Institute of Space Sciences, Cankaya University, Ankara, Magurele, Romania

4 Institute of Space Sciences, Magurele, Romania

5 Department of Applied Mathematics and Statistics, Technical University of Cartagena, Hospital de Marina 30203, Cartagena, Spain

1 Introduction

The historical Emden–Fowler (EF) system is considered very important for the research community because of singularity at the origin and has various applications in wide-ranging fields of applied science and engineering. Some well-known applications are catalytic diffusion reactions using the error estimate models (Burdyny and Smith 2019), stellar configuration (Abbas et al. 2019), density profile of gaseous star (Bacchini et al. 2019), spherical annulus (Soliman 2019), isotropic continuous media (Adel and Sabir 2020), extrinsic thermionic maps (Barilla et al. 2020), the theory of electromagnetic (Guirao et al. 2020) and morphogenesis (Dridi and Trabelsi 2022). Due to the specialty of the singular point and extensive applications, the researcher has always shown keen interest to solve these models all the time. These models are not easy to solve due of this singular model, nonlinearity and stiff nature, and only a few techniques are available in the literature to solve these models. Few of them are Legendre spectral wavelets scheme (Dizicheh et al. 2020), Adomian decomposition scheme (Abdullah Alderremy et al. 2019), Haar quasilinearization wavelet scheme (Singh et al. 2020; Verma and Kumar 2019), an analytic algorithm approach (Arqub et al. 2020), rational Legendre approximation scheme (Dizicheh et al. 2020), modified variational iteration scheme (Verma et al. 2021), differential transformation scheme (Xie et al. 2019), fourth-order B-spline collocation scheme (Roul and Thula 2019), Chebyshev operational matrix scheme (Sharma et al. 2019) and variation of parameters scheme with an auxiliary parameter (Khalifa and Hassan 2019). Beside these, the numerical methodologies introduced in (Abdelrahman and Alharbi 2021; Alharbi et al. 2020; Almatrafi et al. 2021; Lotfy 2019; Sabir 2022a, Sabir et al. 2022c) can be exploited for EF equations-based systems.

All these mentioned schemes have their specific merits/advantages and demerits/imperfections, whereas soft computing stochastic solver is used to manipulate the artificial neural networks (ANNs) strength optimized by global/local search proficiencies of particle swarm optimization (PSO) and interior-point method (IPM), i.e., ANNs-PSO-IPM, have not been implemented for the nonlinear coupled EF model of second kind. The researchers have been generally practiced the numerical computing meta-heuristic schemes along with the neural network strengths for solving the various mathematical linear/nonlinear models (Guerrero-Sánchez et al. 2021; Guirao et al. 2022; Lu et al. 2019, 2021; Mehmood et al. 2020; Sabir et al. 2020a, e). Few recent applications of the stochastic solvers are financial market forecasting (Bukhari et al. 2020), food chain model (Sabir 2022b), nonlinear smoking models (Saeed et al. 2022), nonlinear fractional Lane–Emden systems (Sabir et al. 2022d), nonlinear second-order Lane–Emden pantograph delay differential systems (Nisar et al. 2021), peristaltic motion of a third-grade fluid involving planar channel (Mahmood et al. 2022), nonlinear predator–prey system (Umar et al. 2019), elliptic partial differential model (Fateh et al. 2019), mathematical form of the Leptospirosis system (Botmart et al. 2022), HIV mathematical models (Sabir et al. 2021c, 2022a), nonlinear multiple singularity-based systems (Raja et al. 2019), singular Thomas–Fermi equation (Sabir et al. 2018), heartbeat dynamics (Malešević et al. 2020), a corneal model for eye surgery (Umar et al. 2019; Wang et al. 2022) and heat conduction model of the human head (Raja et al. 2018). These proposed stochastic solvers verified the values of the exactness, convergence, and accurateness of the ANNs-PSO-IPM.

Keeping in view all the consequences of above proposals, authors are interested to exploit the numerical stochastic solvers for consistent, stable, and efficient scheme for nonlinear second-order coupled EF system. The literature form of the coupled EF model of second kind is written as (Sabir et al. 2020b):

$$\begin{cases} \dfrac{d^2U}{d\Psi^2} + \dfrac{\alpha}{\Psi}\dfrac{dU}{d\Psi} + H_1(\Psi)G_1(U,V) = F_1(\Psi), \quad U(0) = A, \\ \dfrac{dU(0)}{d\Psi} = 0, \\ \dfrac{d^2V}{d\Psi^2} + \dfrac{\beta}{\Psi}\dfrac{dV}{d\Psi} + H_2(\Psi)G_2(U,V) = F_2(\Psi), \quad V(0) = B, \\ \dfrac{dV(0)}{d\Psi} = 0, \end{cases} \tag{1}$$

where G_1 and G_2 are the nonlinear functions, α and β are the constants, while F_1 and F_2 are designated as a source functions. The aim of this current study is to solve the model given in Eq. (1) through intelligent computing schemes based on ANN-PSO-IP scheme. Some inventive inspiration of the current study is presented as:

- A neuro-swarm novel intelligent computing ANNs-PSO-IPM is designed and presented to solve second-order nonlinear coupled EF model.
- The overlapping results of the proposed ANNs-PSO-IPM with the exact solutions for four different examples of the nonlinear-coupled EF-based model of second kind establish the consistency, exactness and convergence.
- Ratification of the precise performance is authenticated via statistical calculations/observations on multiple runs of ANN-PSO-IP scheme in terms of root mean square error, Variance Account For, Semi Interquartile Range and Theil's inequality coefficient metrics.
- Beside essentially precise continuous results on whole interval, ease in the concept, stability, the smooth implementable practice and extendibility are well-intentioned declarations for the presented ANNs-PSO-IPM.

The remaining forms of the present work are shown as; Sec 2 presents the detailed methodology of the neural networks using the optimization process ANNs-PSO-IP scheme. Sec 3 presents the performance measures. Sec 4 indicates the numerical measures of the ANNs-PSO-IPM together with the statistical measures. Finally, some concluding remarks along with future work plans are described.

2 Methodology

This section presents the design of ANNs-PSO-IPM for second-order nonlinear coupled EF model in two stages as given below:

Stage 1: A mean square error-based objective/fitness function is constructed for nonlinear coupled EF model

Stage 2: The training/learning of the networks is presented with the help of hybrid PSO-IPM.

2.1 ANNs modeling

The neural networks are extensively applied to solve the diverse applications arising in sundry domains of engineering and applied sciences (Nasirzadehroshenin et al. 2020; Sabir et al. 2021b, 2022e; Umar et al. 2020). The proposed results are indicated as $\hat{U}(\Psi)$ and $\hat{V}(\Psi)$, while $\frac{d^n\hat{U}}{d\Psi^n}$ and $\frac{d^n\hat{V}}{d\Psi^n}$ are the derivatives of n[th] order, respectively, and are given as follows:

$$\begin{aligned}
\left[\hat{U}(\Psi),\,\hat{V}(\Psi)\right] &= \left[\sum_{i=1}^{m}\phi_{U,i}P(w_{U,i}\Psi + a_{U,i}),\right.\\
&\qquad \left.\sum_{i=1}^{m}\phi_{V,i}P(w_{V,i}\Psi + a_{V,i})\right],\\
\left[\frac{d^n\hat{U}}{d\Psi^n},\frac{d^n\hat{V}}{d\Psi^n}\right] &= \left[\sum_{i=1}^{m}\phi_{U,i}\frac{d^n}{d\Psi^n}P(w_{U,i}\Psi + a_{U,i}),\right.\\
&\qquad \left.\sum_{i=1}^{m}\phi_{V,i}\frac{d^n}{d\Psi^n}P(w_{V,i}\Psi + a_{V,i})\right],
\end{aligned} \tag{2}$$

where ϕ, w and a are the unknown weight vectors, while m and n are the number of neurons and the order of derivative, respectively.

$\boldsymbol{W} = [\boldsymbol{W}_U,\,\boldsymbol{W}_V]$, for $\boldsymbol{W}_U = [\boldsymbol{\phi}_U, \boldsymbol{w}_U, \boldsymbol{\alpha}_U]$ and $\boldsymbol{W}_V = [\boldsymbol{\phi}_V, \boldsymbol{w}_V, \boldsymbol{\alpha}_V]$. The weight vector components are shown as:

$$\begin{aligned}
\boldsymbol{\phi}_U &= [\phi_{U,1}, \phi_{U,2}, \cdots, \phi_{U,m}], \quad \boldsymbol{w}_U = [w_{U,1}, w_{U,2}, \cdots, w_{U,m}],\\
&\qquad \boldsymbol{a}_U = [a_{U,1}, a_{U,2}, \cdots, a_{U,m}],\\
\boldsymbol{\phi}_V &= [\phi_{V,1}, \phi_{V,2}, \cdots, \phi_{V,m}], \quad \boldsymbol{w}_V = [w_{V,1}, w_{V,2}, \cdots, w_{V,m}],\\
&\qquad \boldsymbol{a}_V = [a_{V,1}, a_{V,2}, \cdots, a_{V,m}].
\end{aligned}$$

The log-sigmoid $P(\Psi) = \frac{1}{(1+e^{-\Psi})}$ is as an activation function and the simplified form of the network (2) using the $\hat{U}(\Psi)$ and $\hat{V}(\Psi)$ along with their derivatives are shown as:

$$\begin{aligned}
\left[\hat{U}(\Psi),\,\hat{V}(\Psi)\right] &= \left[\sum_{i=1}^{m}\frac{\phi_{U,i}}{1+e^{-\left(w_{U,i}\Psi + a_{U,i}\right)}},\ \sum_{i=1}^{m}\frac{\phi_{V,i}}{1+e^{-\left(w_{V,i}\Psi + a_{V,i}\right)}}\right],\\
\left[\frac{d\hat{U}}{d\Psi},\frac{d\hat{V}}{d\Psi}\right] &= \left[\sum_{i=1}^{m}\frac{\phi_{U,i}w_{U,i}e^{-\left(w_{U,i}\Psi + a_{U,i}\right)}}{\left(1+e^{-\left(w_{U,i}\Psi + a_{U,i}\right)}\right)^2},\ \sum_{i=1}^{m}\frac{\phi_{V,i}w_{V,i}e^{-\left(w_{V,i}\Psi + a_{V,i}\right)}}{\left(1+e^{-\left(w_{V,i}\Psi + a_{V,i}\right)}\right)^2}\right],\\
\left[\frac{d^2\hat{U}}{d\Psi^2},\frac{d^2\hat{V}}{d\Psi^2}\right] &= \left[\begin{array}{l}
\sum_{i=1}^{m}\phi_{U,i}w_{U,i}^2\left\{\frac{2e^{-2\left(w_{U,i}\Psi + a_{U,i}\right)}}{\left(1+e^{-\left(w_{U,i}\Psi + a_{U,i}\right)}\right)^3} - \frac{e^{-\left(w_{U,i}\Psi + a_{U,i}\right)}}{\left(1+e^{-\left(w_{U,i}\Psi + a_{U,i}\right)}\right)^2}\right\},\\
\sum_{i=1}^{m}\phi_{V,i}w_{V,i}^2\left\{\frac{2e^{-2\left(w_{V,i}\Psi + a_{V,i}\right)}}{\left(1+e^{-\left(w_{V,i}\Psi + a_{V,i}\right)}\right)^3} - \frac{e^{-\left(w_{V,i}\Psi + a_{V,i}\right)}}{\left(1+e^{-\left(w_{V,i}\Psi + a_{V,i}\right)}\right)^2}\right\}
\end{array}\right].
\end{aligned} \tag{3}$$

The mean square error-based objective/fitness formulation is formulated as follows:

$$E_{Fit} = E_{Fit-1} + E_{Fit-2} + E_{Fit-3}, \tag{4}$$

$$E_{Fit-1} = \frac{1}{N}\sum_{m=1}^{N}\left(\Psi_m\frac{d^2\hat{U}}{d\Psi_m^2} + \alpha\frac{d\hat{U}}{d\Psi_m} + \Psi_m H_1 G_1(\hat{U},\hat{V}) - \Psi_m F_1\right)^2, \tag{5}$$

$$E_{Fit-2} = \frac{1}{N}\sum_{m=1}^{N}\left(\Psi_m\frac{d^2\hat{V}}{d\Psi_m^2} + \beta\frac{d\hat{V}}{d\Psi_m} + \Psi_m H_2 G_2(\hat{U},\hat{V}) - \Psi_m F_2\right)^2, \tag{6}$$

$$E_{Fit-3} = \frac{1}{6}\left(\left(\hat{U} - A_1\right)^2 + \left(\frac{d\hat{U}}{d\Psi_m}\right)^2 + \left(\hat{V} - A_2\right)^2 + \left(\frac{d\hat{V}}{d\Psi_m}\right)^2\right), \tag{7}$$

where $hN = 1$, $\Psi_m = mh$, $F_1(\Psi) = F_1$ and $F_2(\Psi) = F_2$. The objective functions E_{Fit-1} and E_{Fit-2} are linked with coupled differential systems, and E_{Fit-3} is used for the initial conditions.

2.2 Optimization: PSO-IPM

The optimization to solve the second-order nonlinear-coupled EF system is ratified by the hybrid-computing of PSO-IPM.

PSO is a well-organized search algorithm used as a global search methodology like genetic algorithms (GAs). The PSO algorithm introduced by Eberhart and Kennedy (Hussain and Ismail 2020; Sibalija 2019) and works as an easy procedure that needs minor memory. In search space, an applicant single solution of decision variables by applying optimization is known as a particle and these particles set formulate a swarm. The PSO operates via local $\boldsymbol{P}_{LB}^{\rho-1}$ and global $\boldsymbol{P}_{GB}^{\rho-1}$ best particle positions in a swarm. The position $\mathbf{X}_i$ and velocity $\boldsymbol{V}_i$ are mathematical expressed as follows:

$$\boldsymbol{X}_i^{\chi} = \boldsymbol{V}_i^{\chi-1} + \boldsymbol{X}_i^{\chi-1}, \tag{8}$$

$$\boldsymbol{V}_i^{\chi} = \sigma \boldsymbol{V}_i^{\chi-1} + \xi_1(\boldsymbol{P}_{LB}^{\chi-1} - \boldsymbol{X}_i^{\chi-1})\gamma_1 + \xi_2(\boldsymbol{P}_{GB}^{\chi-1} - \boldsymbol{X}_i^{\chi-1})\gamma_2, \tag{9}$$

here χ stands for iteration/flight index, σ is for inertia weight vector varying between [0. 1], ξ_1 and ξ_2 are the cognitive/social constant accelerations, while, γ_1 and γ_2 are the vectors lie between [0, 1]. Some recent applications of PSO are parameter estimation (Özsoy et al. 2020), robotics (Mai et al. 2019; Yang et al. 2019), nonlinear electric circuits (Qu et al. 2020), systems of equation-based physical models (Kuntoji et al. 2020), and optimization of permanent magnets synchronous motor (Mesloub et al. 2020).

The convergence performance of PSO quickly achieved by using the combination with local search procedure by taking the global best particle of PSO as an initial weight. Consequently, an operative and quick local search approach named as interior-point method (IPM) is oppressed for rapid refinement of the outcomes obtained via PSO scheme. The integrated heuristics of PSO-IPM is exploited to train the networks, while the essential parameter settings of importance elements for PSO-IPM are given in Table 1. Few recently IP scheme applications are power flow security constraint optimization (Casacio et al. 2019), image processing (Chouzenoux et al. 2020), multistage nonlinear nonconvex problems (Zanelli et al. 2020) and nonlinear benchmark models (Wambacq et al. 2021). The PSO-IP scheme is used to train the networks as per process and parameter settings provided in Table 1.

3 Performance indices/metrics

The performances is measured using RMSE, VAF, TIC indices along their globals, i.e., mean values. The mathematical forms of these statistical operatives are given as:

$$[\mathrm{RMSE}_U, \mathrm{RMSE}_V] = \left[\sqrt{\frac{1}{n}\sum_{k=1}^{n}\left(U_k - \hat{U}_k\right)^2}, \sqrt{\frac{1}{n}\sum_{k=1}^{n}\left(V_k - \hat{V}_k\right)^2}\right], \tag{10}$$

$$[\mathrm{TIC}_U, \mathrm{TIC}_V] = \left[\frac{\sqrt{\frac{1}{n}\sum_{k=1}^{n}\left(U(\Psi_k) - \hat{U}(\Psi_k)\right)^2}}{\left(\sqrt{\frac{1}{n}\sum_{k=1}^{n}U^2(\Psi_k)} + \sqrt{\frac{1}{n}\sum_{k=1}^{n}\hat{U}^2(\Psi_k)}\right)}, \frac{\sqrt{\frac{1}{n}\sum_{k=1}^{n}\left(V(\Psi_k) - \hat{V}(\Psi_k)\right)^2}}{\left(\sqrt{\frac{1}{n}\sum_{k=1}^{n}V^2(\Psi_k)} + \sqrt{\frac{1}{n}\sum_{k=1}^{n}\hat{V}^2(\Psi_k)}\right)}\right], \tag{11}$$

$$\begin{cases} [\mathrm{VAF}_U, \mathrm{VAF}_V] = \left[\left(1 - \frac{\mathrm{var}\left(U(\Psi_k) - \hat{U}(\Psi_k)\right)}{\mathrm{var}(U(\Psi_k))}\right) \times 100, \left(1 - \frac{\mathrm{var}\left(V(\Psi_k) - \hat{V}(\Psi_k)\right)}{\mathrm{var}(V(\Psi_k))}\right) \times 100\right], \\ [\mathrm{EVAF}_U, \mathrm{EVAF}_V] = [|VAF_U - 100|, |VAF_V - 100|]. \end{cases} \tag{12}$$

4 Results and discussions

The detail for presenting the solving the four examples of second-order coupled EF model is presented in this section.

Problem I Consider the second-order nonlinear-coupled EF model is given as:

$$\begin{cases} \frac{d^2U}{d\Psi^2} + \frac{1}{\Psi}\frac{dU}{d\Psi} - (4\Psi^2+5)U = 0, \quad U(0)=1, \ \frac{dU(0)}{d\Psi} = 0, \\ \frac{d^2V}{d\Psi^2} + \frac{2}{\Psi}\frac{dV}{d\Psi} - (4\Psi^2-5)V = 0, \quad V(0)=1, \ \frac{dV(0)}{d\Psi} = 0. \end{cases} \tag{13}$$

The exact solutions of Eq. (13) are $[e^{\Psi^2}, \ e^{-\Psi^2}]$, whereas the fitness function becomes as:

$$E_{Fit} = \frac{1}{N}\sum_{m=0}^{N}\left(\begin{array}{c} \left(\Psi_m\frac{d^2\hat{U}}{d\Psi_m^2} + \frac{d\hat{U}}{d\Psi_m} - \Psi_m(4\Psi_m^2+5)\hat{U}\right)^2 + \\ \left(\Psi_m\frac{d^2\hat{V}}{d\Psi_m^2} + 2\frac{d\hat{V}}{d\Psi_m} - \Psi_m(4\Psi_m^2-5)\hat{V}\right)^2 \end{array}\right) + \frac{1}{4}\left(\begin{array}{c} (\hat{U}-1)^2 + \left(\frac{d\hat{U}}{d\Psi_m}\right)^2 \\ +(\hat{V}-1)^2 + \left(\frac{d\hat{V}}{d\Psi_m}\right)^2 \end{array}\right), \tag{14}$$

here N =20, 25 and 30 for input span [0, 1], [0, 1.25] and [0, 1.5], respectively.

Problem II Consider the second-order nonlinear-coupled EF system is written as:

$$\begin{cases} \frac{d^2U}{d\Psi^2} + \frac{2}{\Psi}\frac{dU}{d\Psi} - U^2 + V^2 + 6V = 6\Psi^2 + 6, \\ U(0) = 1, \ \frac{dU(0)}{d\Psi} = 0, \\ \frac{d^2V}{d\Psi^2} + \frac{2}{\Psi}\frac{dV}{d\Psi} + U^2 - V^2 - 6V = -6\Psi^2 + 6, \\ V(0) = -1, \ \frac{dV(0)}{d\Psi} = 0. \end{cases} \tag{15}$$

The exact solutions of Eq. (15) are $\left[\Psi^2 + e^{\Psi^2}, \Psi^2 - e^{\Psi^2}\right]$, and the error function is given as:

$$E_{Fit} = \frac{1}{N}\sum_{m=0}^{N}\left(\begin{array}{c} \left(\Psi_m\frac{d^2\hat{U}}{d\Psi_m^2} + 2\frac{d\hat{U}}{d\Psi_m} - \Psi_m\hat{U}^2 + \Psi_m\hat{V}^2 + 6\Psi_m\hat{V} = 6\Psi_m^3 + 6\Psi_m\right)^2 + \\ \left(\Psi_m\frac{d^2\hat{V}}{d\Psi_m^2} + 2\frac{d\hat{V}}{d\Psi_m} + \Psi_m\hat{U}^2 - \Psi_m\hat{V}^2 - 6\Psi_m\hat{V} = -6\Psi_m^3 + 6\Psi_m\right)^2 \end{array}\right) + \frac{1}{4}\left((\hat{U}-1)^2 + \left(\frac{d\hat{U}}{d\Psi_m}\right)^2 + (\hat{V}+1)^2 + \left(\frac{d\hat{V}}{d\Psi_m}\right)^2\right), \tag{16}$$

here, N =20, 25 and 30 for input span [0, 1], [0, 1.25] and [0, 1.5], respectively.

Problem III Consider the second-order nonlinear-coupled EF model is given as:

$$\begin{cases} \frac{d^2U}{d\Psi^2} + \frac{3}{\Psi}\frac{dU}{d\Psi} - 4(U+V) = 0, \quad U(0)=1, \ \frac{dU(0)}{d\Psi} = 0, \\ \frac{d^2V}{d\Psi^2} + \frac{2}{\Psi}\frac{dV}{d\Psi} + 3(U+V) = 0, \quad V(0)=1, \ \frac{dV(0)}{d\Psi} = 0. \end{cases} \tag{17}$$

The exact solutions of Eq. (17) are $\left[1+\Psi^2, \ 1-\Psi^2\right]$, and the fitness/objective function is given as follows:

$$E_{Fit} = \frac{1}{N}\sum_{m=0}^{N}\left(\begin{array}{c} \left(\Psi_m\frac{d^2\hat{U}}{d\Psi_m^2} + 3\frac{d\hat{U}}{d\Psi_m} - 4\Psi_m(\hat{U}+\hat{V})\right)^2 + \\ \left(\Psi_m\frac{d^2\hat{V}}{d\Psi_m^2} + 2\frac{d\hat{V}}{d\Psi_m} + 3\Psi_m(\hat{U}+\hat{V})\right)^2 \end{array}\right) + \frac{1}{4}\left(\begin{array}{c} (\hat{U}-1)^2 + \left(\frac{d\hat{U}}{d\Psi_m}\right)^2 \\ +(\hat{V}-1)^2 + \left(\frac{d\hat{V}}{d\Psi_m}\right)^2 \end{array}\right). \tag{18}$$

here N =20, 25 and 30 for input span [0, 1], [0, 1.25] and [0, 1.5], respectively.

Problem IV Consider the second-order nonlinear-coupled EF model is given as:

$$\begin{cases} \frac{d^2U}{d\Psi^2} + \frac{1}{\Psi}\frac{dU}{d\Psi} - (1+U^2)V^3 = 0, \quad U(0)=1, \quad \frac{dU(0)}{d\Psi} = 0, \\ \frac{d^2V}{d\Psi^2} + \frac{3}{\Psi}\frac{dV}{d\Psi} + (3+U^2)V^5 = 0, \quad V(0)=1, \quad \frac{dV(0)}{d\Psi} = 0. \end{cases} \tag{19}$$

The exact solutions of Eq. (17) are $\left[\sqrt{1+\Psi^2}, \ \frac{1}{\sqrt{1+\Psi^2}}\right]$, and the fitness/objective function is given as follows:

$$E_{Fit} = \frac{1}{N}\sum_{m=0}^{N}\left(\begin{array}{c}\left(\Psi_m \frac{d^2\hat{U}}{d\Psi_m^2} + \frac{d\hat{U}}{d\Psi_m} - \hat{V}^3\Psi_m(\hat{U}^2+1)\right)^2 + \\ \left(\Psi_m \frac{d^2\hat{V}}{d\Psi_m^2} + 3\frac{d\hat{V}}{d\Psi_m} + \hat{V}^5\Psi_m(\hat{U}^2+3)\right)^2\end{array}\right) + \frac{1}{4}\left(\begin{array}{c}(\hat{U}-1)^2 + \left(\frac{d\hat{U}}{d\Psi_m}\right)^2 \\ +(\hat{V}-1)^2 + \left(\frac{d\hat{V}}{d\Psi_m}\right)^2\end{array}\right), \tag{20}$$

here N =20, 25 and 30 for input span [0, 1], [0, 1.25] and [0, 1.5], respectively.

To calculate/determined the proposed numerical outcomes for the Problems I to IV based on the second-order nonlinear-coupled EF model using the proposed PSO-IPM executed for 50 multiple runs to attain the adjustable weights. The numerical values of the weights are presented in Fig. 1 for $\hat{U}$ and $\hat{V}$. These parameters are applied to get the estimated results for all four variants based on the second-order nonlinear-coupled EF model and the mathematical representations becomes as:

Fig. 1 Best weight sets and results comparison for all the Problems of second-order nonlinear-coupled EF model ▶

$$\begin{aligned}\hat{U}_{P-I} = & \frac{1.6758}{1+e^{-(1.425\Psi+1.998)}} - \frac{3.8309}{1+e^{-(-4.376\Psi+5.970)}} \\ & + \frac{2.3451}{1+e^{-(1.5452\Psi-3.003)}} + \cdots \\ & - \frac{6.8234}{1+e^{-(-7.387\Psi+11.211)}},\end{aligned} \tag{21}$$

$$\begin{aligned}\hat{U}_{P-II} = & \frac{6.0315}{1+e^{-(0.578\Psi+0.192)}} + \frac{9.0343}{1+e^{-(6.155\Psi-9.503)}} \\ & + \frac{1.297}{1+e^{-(-2.206\Psi-1.560)}} + \cdots \\ & + \frac{4.6126}{1+e^{-(-2.220\Psi-1.921)}},\end{aligned} \tag{22}$$

Table 1 Comprehensive pseudocode of PSO-IP scheme for solving the second-order nonlinear coupled EF model

```
PSO algorithm start
Step 1: Initialization: Create the prime swarm arbitrarily and initialize the
parameters of PSO routine and optimoptions tool.
Step-2: Fitness Assessment: Determine/Analyze the fitness of each particle in
the swarm using equations (4) to (7).
Step-3: Rank of particle: Ranking is associated for each particle of swarm
via minimum criteria of the fitness/objective function.
Step-4: Stoppage Criteria: Terminate, if one of below standard meets
      • Fitness level
      • Selected flights
When the above standard accomplished, then go to Step 5
Step-5: Modification: Update the position and velocity by using expressions
(8) and (9), respectively.
Step-6: Repetition: Repeat steps 2 to 6 till the whole flights are completed.
Step-7: Storage: The parameters of global best particle are store along with
its fitness.
PSO algorithm stop
Start of PSO-IP scheme
Inputs:  'global best particle' of PSO
Output: W_PSOIP are the 'PSOIP's trained weights
Initialization: Use 'global best particle' as a start point of IPM.
Termination: Stop the execution, when one of the below conditions meet
[Fitness = E_Fit = 10^-20], [TolX = 10^-21], [Generation =  1000],    [TolFun    =
TolCon = 10^-22] and [MaxFunEvals = 265000]
While [Terminate]
Fitness Evaluation: The set (4) is applied for the 'fitness value'
Adjustments: Invoke the 'fmincon' routine for the IP scheme to regulate the
'weight vector' values.
Store the 'fitness values' using the 'basic form' of the 'weight vector'
Store:  W_PSO-IP  scheme  values,  best  weights,  fitness,  function  count,
generations and time for the current run.
PSO-IP scheme End
```

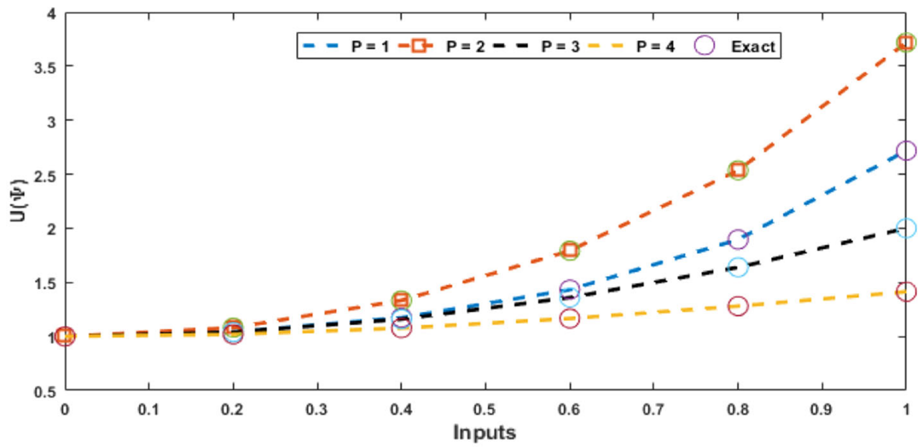

(a) Results of $\hat{U}(\Psi)$ for Problems I to IV

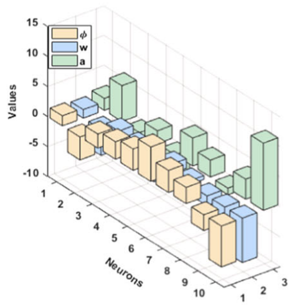

(b) P-I weights for $\hat{U}(\Psi)$

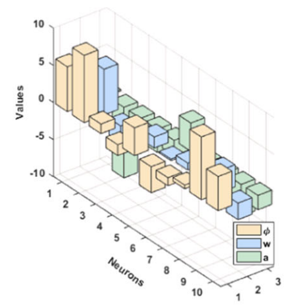

(c) P- IIweights for $\hat{U}(\Psi)$

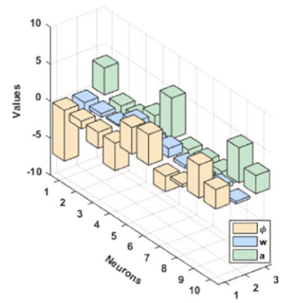

(d) P-III weights for $\hat{U}$ (Ψ)

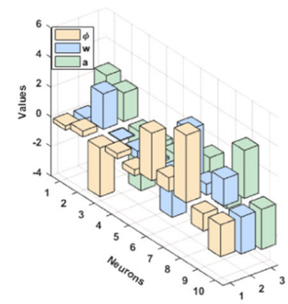

(e) P-IV weights for $\hat{U}$ (Ψ)

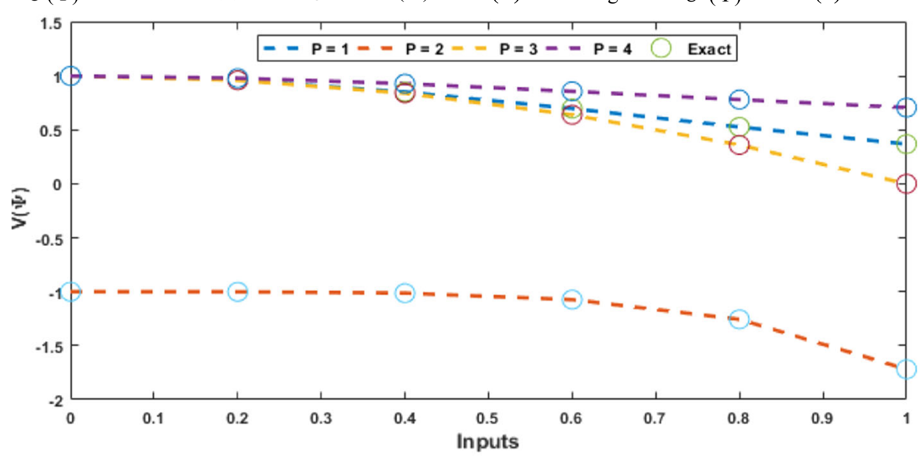

(f) Results of $\hat{V}$ (Ψ) for Problems I to IV

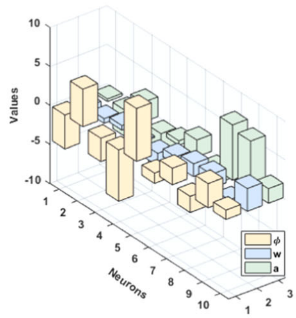

(g) P-I weights for $\hat{V}$ (Ψ)

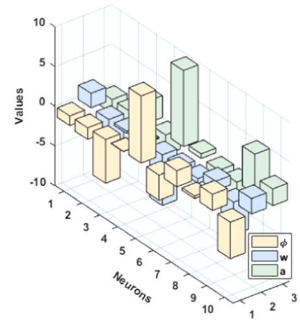

(h) P-II weights for $\hat{V}$ (Ψ)

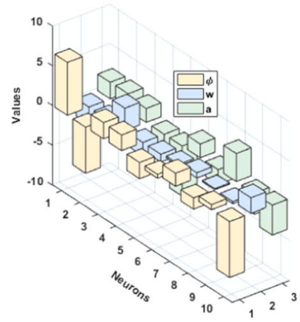

(i) P-III weights for $\hat{V}$ (Ψ)

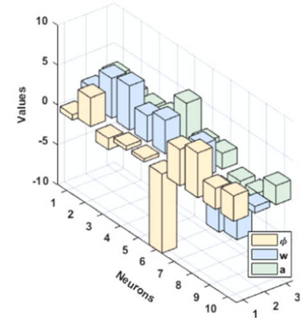

(j): P-IV weights for $\hat{V}(\Psi)$

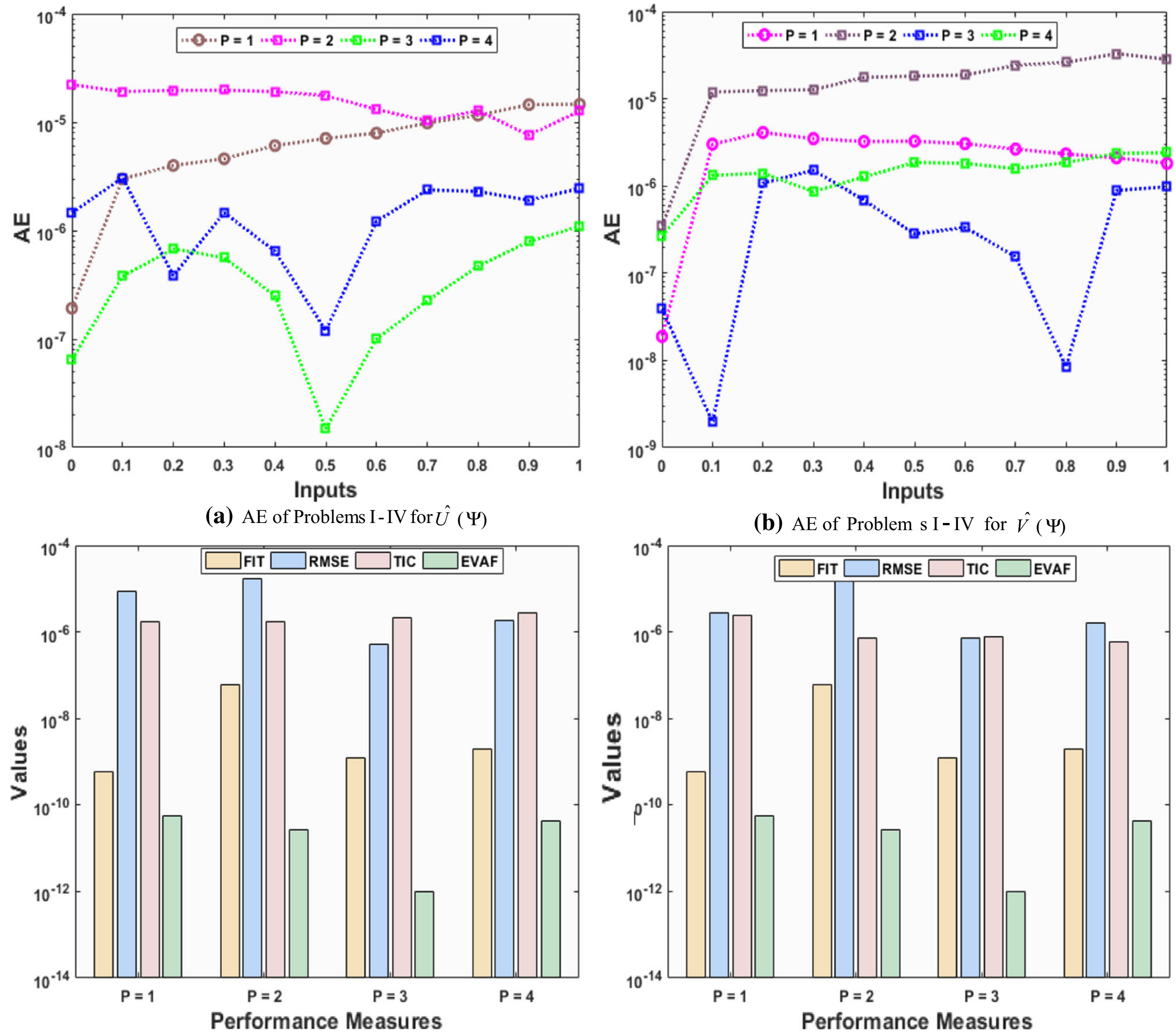

(a) AE of Problems I-IV for $\hat{U}(\Psi)$ **(b)** AE of Problem s I-IV for $\hat{V}(\Psi)$

(c) Performance indices of Problem I-IV for $\hat{U}(\Psi)$ **(d)** Performance indices of Problem I-IV for $\hat{V}(\Psi)$

Fig. 2 Absolute error and performance measures for all Problems of second-order nonlinear-coupled EF model

$$\begin{aligned}\hat{U}_{P-III} = &\frac{-6.8663}{1+e^{-(-1.574\Psi+3.654)}} - \frac{1.0189}{1+e^{-(-0.492\Psi-1.299)}} \\ &- \frac{2.1697}{1+e^{-(-0.194\Psi-4.339)}} + \cdots \\ &+ \frac{2.6387}{1+e^{-(-0.331\Psi+2.246)}},\end{aligned} \tag{23}$$

$$\begin{aligned}\hat{U}_{P-IV} = &\frac{-0.2821}{1+e^{-(-0.533\Psi+2.368)}} + \frac{0.3969}{1+e^{-(2.391\Psi+1.929)}} \\ &- \frac{3.3036}{1+e^{-(-0.038\Psi-3.927)}} + \cdots \\ &- \frac{2.1545}{1+e^{-(-2.484\Psi-2.701)}},\end{aligned} \tag{24}$$

$$\begin{aligned}\hat{V}_{P-I} = &\frac{-4.3366}{1+e^{-(-1.990\Psi-0.338)}} + \frac{4.8079}{1+e^{-(-0.598\Psi-3.336)}} \\ &- \frac{2.9912}{1+e^{-(0.600\Psi+2.518)}} + \cdots + \frac{1.1862}{1+e^{-(2.928\Psi+1.879)}},\end{aligned} \tag{25}$$

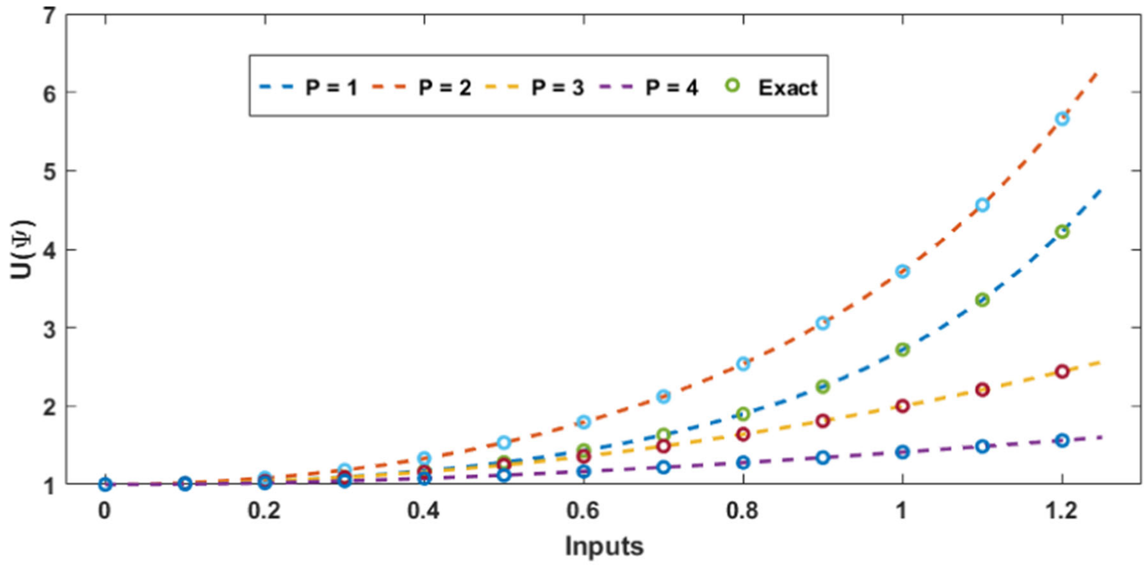

(a) results for U (Ψ)

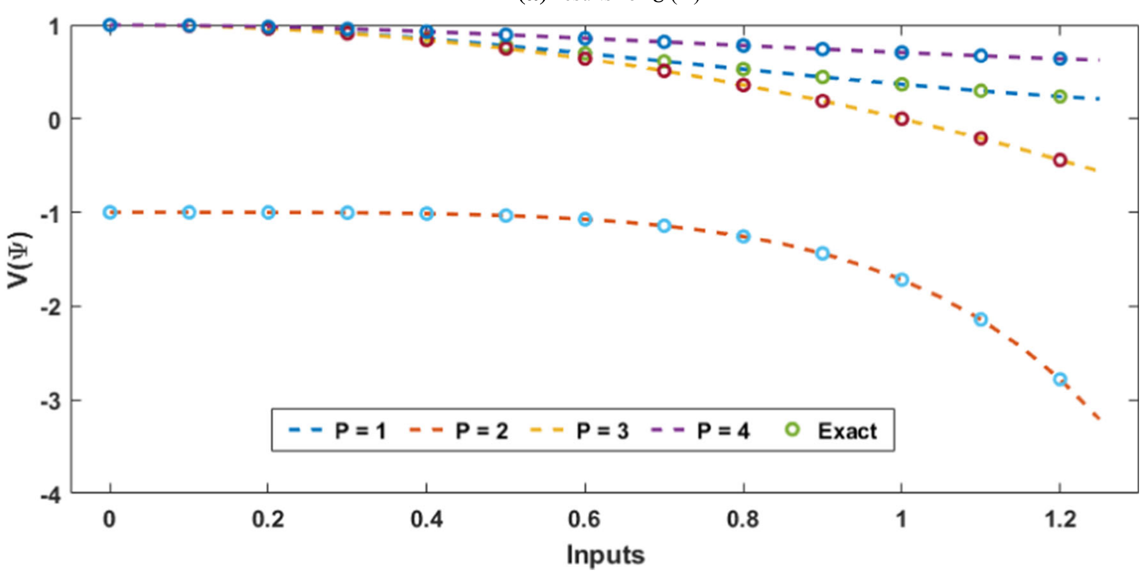

(b) results for V (Ψ)

Fig. 3 Comparison of proposed solutions for all Problems of second-order nonlinear-coupled EF model in case of input interval [0, 1.25]

$$\begin{aligned}\hat{V}_{P-II} = &\frac{-1.2095}{1+e^{-(1.812\Psi-1.701)}} - \frac{1.4677}{1+e^{-(-3.875\Psi-2.842)}} \\ &- \frac{5.4743}{1+e^{-(-0.276\Psi+2.736)}} + \cdots \\ &- \frac{4.5921}{1+e^{-(1.927\Psi+2.108)}},\end{aligned} \tag{26}$$

$$\begin{aligned}\hat{V}_{P-III} = &\frac{2.237}{1+e^{-(0.454\Psi-0.035)}} - \frac{0.825}{1+e^{-(1.564\Psi+0.541)}} \\ &- \frac{0.249}{1+e^{-(1.204\Psi-0.301)}} + \cdots \\ &- \frac{0.7721}{1+e^{-(-1.792\Psi+0.440)}},\end{aligned} \tag{27}$$

$$\begin{aligned}\hat{V}_{P-IV} = &\frac{-0.6548}{1+e^{-(2.202\Psi+2.856)}} + \frac{3.6090}{1+e^{-(5.003\Psi+2.080)}} \\ &- \frac{1.4197}{1+e^{-(5.548\Psi+1.859)}} + \cdots + \frac{3.1940}{1+e^{-(-0.815+2.385)}}.\end{aligned} \tag{28}$$

The optimization is performed for all the problems of the nonlinear-coupled EF system with ANNs-PSO-IPM for 50 independent runs. A set of the best weights along with proposed and exact outcomes are shown in Fig. 1. It is stated that all the problems of the nonlinear-coupled EF system of second kind, the exact/reference solution and ANNs-PSO-IPM results overlapped consistently for $\hat{U}(\Psi)$ and $\hat{V}(\Psi)$. This overlapping of the outcomes depicts the

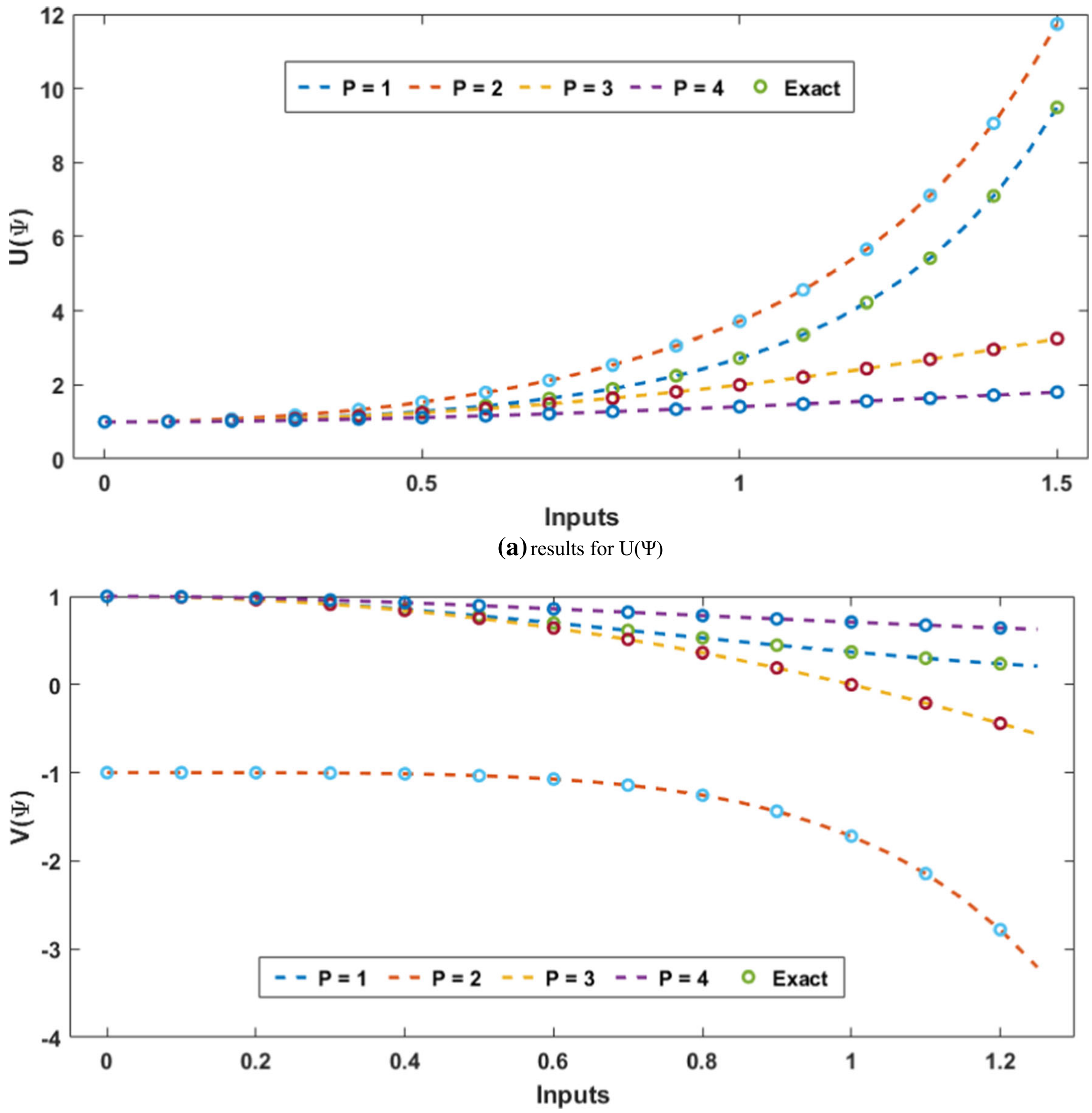

(a) results for U(Ψ)

(b) results for V(Ψ)

Fig. 4 Comparison of proposed solutions for all Problems of second-order nonlinear-coupled EF model in case of input interval [0, 1.5]

correctness/exactness of the proposed ANNs-PSO-IP scheme. Figure 2 shows the absolute error (AE), comparison of the proposed results and exact solutions as well as analysis on different performance metrics. The approximate solutions for $N = 25$ and $N = 30$ are plotted in Figs. 3 and 4 along with the reference exact values. One may see that results are consistently overlapping for small as well as large interval. The AE plots for $\hat{U}(\Psi)$ and $\hat{V}(\Psi)$ are drawn in Fig. 2a and b for $N = 20$, while the performance measures for $\hat{U}(\Psi)$ and $\hat{V}(\Psi)$ are provided in Fig. 2c and d for $N = 20$. It is observed that the AE values of $\hat{U}(\Psi)$ lie around 10^{-05}–10^{-06}, 10^{-04}–10^{-05}, 10^{-06}–10^{-08} and 10^{-06}–10^{-07} for Problem I, II, III and IV in case of $N = 20$, 25 and 30. While the AE values of $\hat{V}(\Psi)$ lie around 10^{-05}–10^{-06}, 10^{-04}–10^{-05}, 10^{-06}–10^{-09} and 10^{-06}–10^{-07} for Problems I–IV for $N = 20$. The performance measures of $\hat{U}(\chi)$ and $\hat{V}(\Psi)$ based on FIT, RMSE, TIIC and EVAF are plotted in Fig. 2c and d. It is seen that the FIT for $\hat{U}(\Psi)$ and $\hat{V}(\Psi)$ lie close to 10^{-08}–10^{-10}, for problems I, III and IV, and similarly the FIT for Problem II lies around 10^{-06}–10^{-08}. The RMSE and TIC for $\hat{U}(\Psi)$ and $\hat{V}(\Psi)$ lie around to 10^{-04}–10^{-06}, for all the problems. The TIC values lie around 10^{-06}–10^{-08} for both indexes of all the Problems. The values of the EVAF for both indices of all the problems lie around 10^{-10}–10^{-12}. The convergence measures for the Problems I–IV based on the second-order nonlinear-coupled EF model using the fitness values, boxplots and histograms with 10 neurons are plotted in

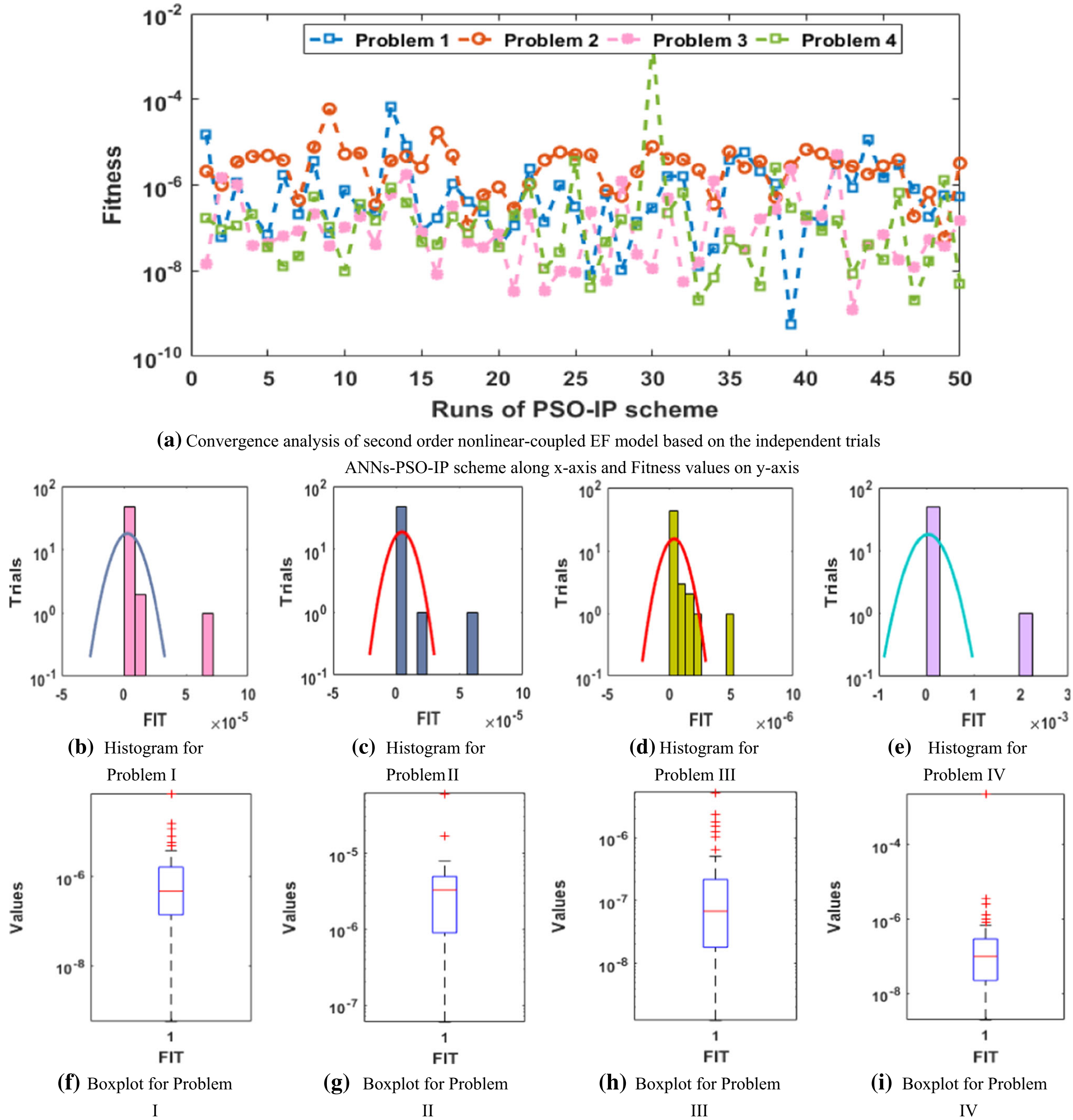

(a) Convergence analysis of second order nonlinear-coupled EF model based on the independent trials ANNs-PSO-IP scheme along x-axis and Fitness values on y-axis

(b) Histogram for Problem I **(c)** Histogram for Problem II **(d)** Histogram for Problem III **(e)** Histogram for Problem IV

(f) Boxplot for Problem I **(g)** Boxplot for Problem II **(h)** Boxplot for Problem III **(i)** Boxplot for Problem IV

Fig. 5 Convergence indices for all the Problems of second-order nonlinear-coupled EF model using the Fitness, boxplots and boxplots for 10 neurons

Fig 5. It is seen that the fitness lies around 10^{-04}–10^{-08} for the Problems I–IV.

For more satisfaction, accuracy and precision examination of the ANNs-PSO-IP scheme, statistical measures are made based on minimum (MIN), mean, standard deviation (SD), median and semi interquartile range (S-IR). S-IR range is 0.5 times of the difference of the third quartile, i.e., Q_3 = 75% data and first quartile, i.e., Q_1 = 25% data, is calculated for 50 runs of ANNs-PSO-IP scheme to solve four different examples of the nonlinear-coupled EF system of second kind. These statistical results for Problems I–IV are provided in Tables 2 as well as 3 for $\hat{U}$ and $\hat{V}$, respectively. It is perceived that both $\hat{U}(\Psi)$ and $\hat{V}(\Psi)$ for Problems I–IV lie in the good range. The global performance, i.e., G-FIT, G-EVAF, G-RMSE and G-TIC

Table 2 Statistics on $\hat{U}(\Psi)$ for all the Problems of second-order nonlinear-coupled EF model using the ANNs-PSO-IP approach

Mode	Solutions of $\hat{U}(\Psi)$ for Problems I to IV between [0,1]										
	0	0.10	0.20	0.30	0.40	0.50	0.60	0.70	0.80	0.90	1.0
Problem I											
Min	3.5×10^{-07}	3.0×10^{-06}	4.0×10^{-06}	4.6×10^{-06}	6.1×10^{-06}	7.0×10^{-06}	7.9×10^{-06}	9.8×10^{-06}	1.2×10^{-05}	1.5×10^{-05}	1.5×10^{-05}
Mean	4.9×10^{-05}	5.7×10^{-03}	8.5×10^{-03}	2.2×10^{-02}	2.4×10^{-02}	2.6×10^{-02}	1.9×10^{-02}	4.7×10^{-02}	3.8×10^{-02}	3.1×10^{-02}	4.9×10^{-02}
SD	2.7×10^{-04}	1.8×10^{-02}	2.4×10^{-02}	5.0×10^{-02}	6.9×10^{-02}	7.9×10^{-02}	6.8×10^{-02}	5.5×10^{-02}	6.5×10^{-02}	$7.8 \times 10-01$	$9.4 \times 10-01$
Median	3.4×10^{-07}	7.5×10^{-04}	2.4×10^{-03}	2.5×10^{-03}	5.9×10^{-05}	3.5×10^{-03}	9.7×10^{-04}	8.1×10^{-05}	3.2×10^{-06}	8.2×10^{-05}	1.9×10^{-05}
SIR	1.7×10^{-05}	8.3×10^{-05}	6.4×10^{-05}	3.5×10^{-04}	2.4×10^{-06}	2.6×10^{-05}	2.4×10^{-04}	3.5×10^{-04}	7.4×10^{-05}	1.9×10^{-05}	6.5×10^{-04}
Problem II											
Min	7.5×10^{-07}	1.3×10^{-06}	4.5×10^{-05}	9.7×10^{-05}	2.0×10^{-07}	1.5×10^{-07}	3.3×10^{-07}	1.0×10^{-05}	2.6×10^{-06}	7.8×10^{-06}	2.6×10^{-07}
Mean	3.9×10^{-05}	9.7×10^{-05}	1.5×10^{-03}	1.5×10^{-04}	3.9×10^{-04}	2.9×10^{-05}	2.0×10^{-04}	2.3×10^{-04}	2.6×10^{-05}	3.1×10^{-05}	3.7×10^{-05}
SD	6.6×10^{-05}	1.1×10^{-04}	1.5×10^{-04}	1.5×10^{-04}	1.5×10^{-04}	1.6×10^{-04}	1.9×10^{-06}	2.1×10^{-03}	2.3×10^{-03}	9.2×10^{-04}	3.3×10^{-05}
Median	9.6×10^{-06}	7.2×10^{-05}	4.5×10^{-05}	1.1×10^{-04}	1.0×10^{-04}	1.1×10^{-04}	1.4×10^{-04}	1.7×10^{-04}	2.1×10^{-04}	3.5×10^{-05}	3.5×10^{-04}
SIR	1.8×10^{-05}	4.7×10^{-05}	2.3×10^{-06}	8.7×10^{-05}	7.2×10^{-05}	7.9×10^{-06}	9.8×10^{-06}	9.5×10^{-05}	1.0×10^{-02}	9.2×10^{-04}	1.9×10^{-05}
Problem III											
Min	1.1×10^{-08}	7.6×10^{-07}	7.8×10^{-07}	6.1×10^{-07}	5.7×10^{-08}	2.6×10^{-08}	2.1×10^{-07}	3.3×10^{-07}	5.6×10^{-07}	5.6×10^{-07}	4.4×10^{-07}
Mean	4.4×10^{-06}	6.9×10^{-06}	3.4×10^{-06}	4.2×10^{-04}	2.9×10^{-07}	4.5×10^{-06}	3.0×10^{-05}	4.3×10^{-06}	3.4×10^{-04}	3.7×10^{-06}	3.2×10^{-06}
SD	6.5×10^{-05}	6.1×10^{-05}	3.8×10^{-05}	3.2×10^{-05}	3.4×10^{-05}	6.1×10^{-04}	4.3×10^{-04}	3.6×10^{-05}	4.2×10^{-03}	4.4×10^{-05}	5.2×10^{-04}
Median	9.6×10^{-06}	3.9×10^{-04}	8.1×10^{-06}	7.2×10^{-06}	7.3×10^{-06}	8.0×10^{-05}	8.7×10^{-05}	6.3×10^{-07}	3.6×10^{-05}	6.2×10^{-04}	1.6×10^{-05}
SIR	2.9×10^{-06}	8.4×10^{-06}	9.5×10^{-04}	9.2×10^{-07}	4.3×10^{-06}	7.3×10^{-06}	4.5×10^{-07}	2.1×10^{-05}	9.1×10^{-06}	3.3×10^{-07}	1.7×10^{-06}
Problem IV											
Min	3.3×10^{-08}	4.4×10^{-07}	6.8×10^{-07}	1.5×10^{-05}	9.2×10^{-07}	3.4×10^{-07}	2.2×10^{-06}	5.4×10^{-06}	5.4×10^{-07}	6.4×10^{-06}	2.2×10^{-06}
Mean	6.5×10^{-04}	1.0×10^{-02}	2.7×10^{-05}	5.1×10^{-03}	3.4×10^{-03}	2.7×10^{-04}	1.2×10^{-04}	6.1×10^{-05}	2.4×10^{-03}	3.6×10^{-04}	3.6×10^{-04}
SD	7.4×10^{-03}	9.3×10^{-03}	4.2×10^{-03}	3.5×10^{-03}	2.6×10^{-02}	2.6×10^{-03}	3.4×10^{-03}	5.2×10^{-03}	4.6×10^{-02}	2.5×10^{-03}	2.6×10^{-03}
Median	4.9×10^{-06}	2.5×10^{-05}	6.2×10^{-05}	5.8×10^{-05}	4.3×10^{-05}	5.4×10^{-05}	5.9×10^{-06}	6.7×10^{-04}	6.0×10^{-05}	8.4×10^{-04}	6.8×10^{-05}
SIR	8.1×10^{-06}	4.9×10^{-06}	9.4×10^{-06}	7.2×10^{-04}	6.6×10^{-06}	4.5×10^{-06}	7.8×10^{-05}	7.4×10^{-05}	7.3×10^{-06}	6.2×10^{-06}	5.4×10^{-06}

Table 3 Statistics on $\hat{V}(\Psi)$ for all Problems of second-order nonlinear-coupled EF model using the ANNs-PSO-IP approach

Mode	Solutions of $\hat{V}(\Psi)$ for Problems I to IV between [0,1] with 0.1 step size										
	0	0.1	0.2	0.3	0.4	0.5	0.6	0.7	0.8	0.9	1
Problem I											
Min	2.7×10^{-08}	8.3×10^{-07}	7.0×10^{-07}	4.6×10^{-07}	2.3×10^{-07}	6.2×10^{-07}	2.3×10^{-07}	2.2×10^{-07}	2.2×10^{-06}	6.0×10^{-07}	4.8×10^{-07}
Mean	3.2×10^{-06}	7.3×10^{-05}	4.2×10^{-04}	2.2×10^{-03}	3.2×10^{-03}	3.5×10^{-03}	5.2×10^{-03}	6.7×10^{-03}	8.8×10^{-03}	2.2×10^{-03}	2.3×10^{-04}
SD	8.4×10^{-04}	2.4×10^{-04}	7.4×10^{-04}	3.6×10^{-03}	5.3×10^{-03}	8.7×10^{-03}	2.3×10^{-03}	2.7×10^{-03}	3.3×10^{-03}	3.7×10^{-03}	3.2×10^{-03}
Median	7.3×10^{-05}	2.7×10^{-05}	3.7×10^{-05}	3.6×10^{-05}	2.7×10^{-05}	2.4×10^{-05}	2.5×10^{-05}	2.8×10^{-05}	2.4×10^{-05}	2.4×10^{-05}	2.5×10^{-06}
SIR	2.0×10^{-06}	2.3×10^{-05}	3.4×10^{-05}	3.5×10^{-05}	2.7×10^{-05}	2.4×10^{-05}	2.6×10^{-05}	2.5×10^{-05}	2.3×10^{-05}	2.5×10^{-05}	2.2×10^{-05}
Problem II											
Min	2.0×10^{-07}	4.0×10^{-06}	3.3×10^{-06}	3.3×10^{-07}	3.2×10^{-06}	5.4×10^{-06}	2.7×10^{-06}	7.5×10^{-07}	2.7×10^{-05}	3.7×10^{-07}	2.3×10^{-05}
Mean	3.0×10^{-05}	2.0×10^{-04}	2.8×10^{-04}	3.0×10^{-04}	2.7×10^{-04}	3.0×10^{-04}	3.3×10^{-04}	3.6×10^{-04}	3.7×10^{-04}	3.4×10^{-04}	3.7×10^{-05}
SD	3.7×10^{-05}	7.7×10^{-05}	2.4×10^{-04}	2.5×10^{-04}	2.4×10^{-04}	2.5×10^{-04}	2.7×10^{-04}	2.7×10^{-04}	3.2×10^{-04}	3.6×10^{-04}	3.0×10^{-04}
Median	3.2×10^{-05}	2.0×10^{-04}	2.5×10^{-04}	2.5×10^{-04}	2.6×10^{-04}	2.8×10^{-04}	3.2×10^{-04}	3.6×10^{-04}	3.7×10^{-04}	3.5×10^{-04}	3.7×10^{-04}
SIR	2.7×10^{-05}	4.8×10^{-05}	2.0×10^{-04}	2.3×10^{-04}	2.3×10^{-04}	2.3×10^{-04}	2.3×10^{-04}	2.6×10^{-04}	2.7×10^{-04}	2.7×10^{-04}	3.3×10^{-04}
Problem III											
Min	2.4×10^{-08}	3.0×10^{-07}	2.2×10^{-06}	2.4×10^{-07}	6.7×10^{-07}	3.8×10^{-07}	3.3×10^{-07}	3.5×10^{-07}	8.4×10^{-07}	3.3×10^{-08}	2.8×10^{-07}
Mean	7.7×10^{-06}	2.6×10^{-05}	3.5×10^{-05}	3.4×10^{-05}	3.0×10^{-05}	2.8×10^{-05}	2.8×10^{-05}	2.8×10^{-05}	2.6×10^{-05}	2.4×10^{-05}	2.4×10^{-06}
SD	2.3×10^{-05}	2.7×10^{-05}	3.8×10^{-05}	3.7×10^{-05}	3.4×10^{-05}	3.0×10^{-05}	2.7×10^{-05}	4.7×10^{-05}	2.7×10^{-05}	2.7×10^{-05}	2.6×10^{-05}
Median	3.8×10^{-06}	8.8×10^{-06}	2.5×10^{-05}	2.3×10^{-05}	2.2×10^{-05}	2.2×10^{-05}	2.2×10^{-05}	2.0×10^{-05}	7.6×10^{-06}	8.2×10^{-06}	7.3×10^{-06}
SIR	4.8×10^{-06}	7.4×10^{-06}	2.4×10^{-05}	2.3×10^{-05}	2.3×10^{-05}	2.2×10^{-05}	2.2×10^{-05}	7.0×10^{-06}	8.0×10^{-06}	7.5×10^{-06}	6.7×10^{-06}
Problem IV											
Min	7.2×10^{-08}	3.7×10^{-08}	2.8×10^{-07}	4.5×10^{-07}	3.3×10^{-07}	2.2×10^{-06}	6.0×10^{-07}	3.4×10^{-08}	2.3×10^{-07}	3.3×10^{-07}	3.3×10^{-07}
Median	7.4×10^{-04}	7.3×10^{-04}	6.3×10^{-04}	4.7×10^{-04}	3.7×10^{-04}	4.5×10^{-05}	3.2×10^{-04}	4.3×10^{-04}	6.3×10^{-04}	7.7×10^{-04}	7.4×10^{-04}
SD	5.2×10^{-03}	4.7×10^{-03}	4.3×10^{-03}	3.3×10^{-03}	2.8×10^{-03}	3.3×10^{-04}	2.4×10^{-03}	3.7×10^{-03}	4.3×10^{-03}	5.6×10^{-03}	6.6×10^{-03}
Median	4.8×10^{-06}	2.2×10^{-05}	2.7×10^{-05}	2.4×10^{-05}	8.2×10^{-06}	8.3×10^{-06}	8.3×10^{-06}	7.7×10^{-06}	3.6×10^{-06}	3.8×10^{-06}	4.4×10^{-06}
SIR	6.7×10^{-06}	2.5×10^{-05}	2.6×10^{-05}	2.2×10^{-05}	7.6×10^{-06}	7.3×10^{-06}	6.5×10^{-06}	5.0×10^{-06}	4.5×10^{-06}	4.7×10^{-06}	4.0×10^{-07}

Table 4 Results for global performance on both $\hat{U}(\Psi)$ and $\hat{V}(\Psi)$ in case of Problems I to IV

Index	Problem	G.FIT		G.RMSE		G.TIC		G.EVAF	
		MAG	Median	MAG	Median	MAG	Median	MAG	Median
$\hat{U}(\Psi)$	1	2.95×10^{-06}	4.71×10^{-07}	2.06×10^{-01}	2.28×10^{-04}	2.77×10^{-02}	4.16×10^{-05}	2.71×10^{-01}	4.20×10^{-08}
	2	4.47×10^{-06}	3.29×10^{-06}	2.15×10^{-04}	1.69×10^{-04}	3.95×10^{-02}	4.27×10^{-05}	1.82×10^{-08}	8.89×10^{-09}
	3	3.73×10^{-07}	6.71×10^{-08}	2.26×10^{-05}	1.01×10^{-05}	5.41×10^{-02}	5.44×10^{-05}	1.80×10^{-09}	1.43×10^{-10}
	4	4.42×10^{-05}	9.90×10^{-08}	2.62×10^{-02}	4.77×10^{-05}	5.87×10^{-02}	6.05×10^{-05}	2.94×10^{-01}	2.22×10^{-08}
$\hat{V}(\Psi)$	1	6.6×10^{-06}	3.1×10^{-07}	6.3×10^{-05}	4.2×10^{-06}	1.9×10^{-05}	9.1×10^{-07}	3.6×10^{-08}	5.8×10^{-09}
	2	3.5×10^{-04}	4.8×10^{-06}	5.1×10^{-02}	2.4×10^{-02}	1.2×10^{-05}	7.3×10^{-06}	3.3×10^{-01}	2.1×10^{-03}
	3	1.7×10^{-06}	3.1×10^{-07}	1.8×10^{-05}	8.1×10^{-06}	1.7×10^{-05}	1.1×10^{-05}	3.2×10^{-09}	9.5×10^{-11}
	4	2.3×10^{-05}	2.1×10^{-07}	5.8×10^{-02}	3.5×10^{-06}	5.8×10^{-03}	7.5×10^{-06}	3.5×10^{-02}	2.5×10^{-03}

of $\hat{U}(\Psi)$ and $\hat{V}(\Psi)$ for Problems I–IV is provided in Table 4. In the said Table, the presentations of the global performance for all problems based on second-order nonlinear-coupled EF model for 50 independent executions are provided. The magnitude as well as median values of each Problems based on the second-order nonlinear-coupled EF model using the indexes $\hat{U}(\Psi)$ and $\hat{V}(\Psi)$ proven good. The time complexity of the proposed scheme ANNs-PSO-IPM for all four problems in terms of time consume for learning of weights of neural network is around 50 ± 25 for $N = 20$, while in case of N = 25 and 30 time consumed are around 55 ± 25 and 60 ± 20, respectively.

5 Conclusion

In this investigation, a reliable, stable, consistent and precise numerical ANNs-PSO-IPM is presented for solving the nonlinear-coupled EF system by using the ANNs strength. The objective function is optimized of these networks using the global as well as local search competences of PSO-IPM. The suggested ANNs-PSO-IPM is viably executed to solve four different examples of the nonlinear-coupled EF system. The detailed, precise and particular presentation is obtained for ANNs-PSO-IPM in terms of AE with steadfast precision that is measured around 4–7 decimals of accurateness of the present reference solutions for all four problems of the nonlinear-coupled EF system of second kind. Furthermore, the statistical clarifications achieved good measures using the Min, standard deviation, Mean, S-IR and Median to check the convergence, robustness and accuracy of the ANNs-PSO-IPM for solving the second-order nonlinear-coupled EF model-based problems I–IV.

6 Future research directions

In the future, one can exploit/explore the knacks of ANNs-PSO-IPM to solve the singular higher order models (Sabir et al. 2020c, d; 2021a), fractional order models (İlhan and Kıymaz 2020; Sabir et al. 2022b; Sulaiman et al. 2019; Touchent et al. 2020; Yokuş and Gülbahar 2019; Ziane et al. 2019) and many other applications of utmost importance (Kouider and Polat 2020; Xie et al. 2020; Xue et al. 2021; Yao 2021).

Funding Open Access funding provided thanks to the CRUE-CSIC agreement with Springer Nature. The authors have not disclosed any funding.

Data availability Enquiries about data availability should be directed to the authors.

Declarations

Conflict of interest The authors have not disclosed any competing interests.

References

Abbas F, Kitanov P, Longo S (2019) Approximate solutions to lane-emden equation for stellar configuration. Appl Math Inf Sci 13:143–152

Abdelrahman MA, Alharbi A (2021) Analytical and numerical investigations of the modified Camassa-Holm equation. Pramana 95(3):1–9

Abdullah Alderremy A, Elzaki TM, Chamekh M (2019) Modified Adomian decomposition method to solve generalized Emden-Fowler systems for singular IVP. Math Problems Eng 2019:1–6

Adel W, Sabir Z (2020) Solving a new design of nonlinear second-order Lane-Emden pantograph delay differential model via Bernoulli collocation method. Eur Phys J Plus 135(5):1–12

Alharbi AR, Almatrafi MB, Lotfy K (2020) Constructions of solitary travelling wave solutions for Ito integro-differential equation arising in plasma physics. Results Phys 19:103533

Almatrafi MB, Alharbi A, Lotfy K, El-Bary AA (2021) Exact and numerical solutions for the GBBM equation using an adaptive moving mesh method. Alex Eng J 60(5):4441–4450

Arqub OA, Osman MS, Abdel-Aty AH, Mohamed ABA, Momani S (2020) A numerical algorithm for the solutions of ABC singular Lane-Emden type models arising in astrophysics using reproducing kernel discretization method. Mathematics 8(6):923

Bacchini C, Fraternali F, Iorio G, Pezzulli G (2019) Volumetric star formation laws of disc galaxies. Astron Astrophys 622:A64

Barilla D, Caristi G, Heidarkhani S, Moradi S (2020) Generalized yamabe equations on riemannian manifolds and applications to Emden-Fowler problems. Quaest Math 43(4):547–567

Botmart T et al (2022) A hybrid swarming computing approach to solve the biological nonlinear Leptospirosis system. Biomed Signal Process Control 77:103789

Bukhari AH et al (2020) Fractional neuro-sequential ARFIMA-LSTM for financial market forecasting. IEEE Access 8:71326–71338

Burdyny T, Smith WA (2019) CO 2 reduction on gas-diffusion electrodes and why catalytic performance must be assessed at commercially-relevant conditions. Energy Environ Sci 12(5):1442–1453

Casacio L, Lyra C, Oliveira AR (2019) Interior point methods for power flow optimization with security constraints. Int Trans Oper Res 26(1):364–378

Chouzenoux E, Corbineau MC, Pesquet JC (2020) A proximal interior point algorithm with applications to image processing. J Math Imag Vis 62(6):919–940

Dizicheh AK, Salahshour S, Ahmadian A, Baleanu D (2020) A novel algorithm based on the Legendre wavelets spectral technique for solving the Lane-Emden equations. Appl Numer Math 153:443–456

Dridi A, Trabelsi N (2022) Blow up solutions for a 4-dimensional Emden-Fowler system of Liouville type. J Elliptic Parabolic Equ 8:331–366

Fateh MF et al (2019) Differential evolution based computation intelligence solver for elliptic partial differential equations. Front Inf Technol Electron Eng 20(10):1445–1456

Guerrero-Sánchez Y, Umar M, Sabir Z, Guirao JL, Raja MAZ (2021) Solving a class of biological HIV infection model of latently infected cells using heuristic approach. Discr Contin Dyn Syst-S 14(10):3611

Guirao JL, Sabir Z, Saeed T (2020) Design and numerical solutions of a novel third-order nonlinear Emden-Fowler delay differential model. Math Problems Eng 2020:1–9

Guirao JL, Sabir Z, Raja MAZ, Baleanu D (2022) Design of neuro-swarming computational solver for the fractional Bagley-Torvik mathematical model. Eur Phys J Plus 137(2):245

Hussain AN, Ismail AA (2020) Operation cost reduction in unit commitment problem using improved quantum binary PSO algorithm. Int J Electr Comput Eng 10:1149–1155

İlhan E, Kıymaz İO (2020) A generalization of truncated M-fractional derivative and applications to fractional differential equations. Appl Math Nonlinear Sci 5(1):171–188

Khalifa AS, Hassan HN (2019) Approximate solution of Lane-Emden type equations using variation of parameters method with an auxiliary parameter. J Appl Math Phys 7(04):921

Kouider B, Polat A (2020) Optimal position of piezoelectric actuators for active vibration reduction of beams. Appl Math Nonlinear Sci 5(1):385–392

Kuntoji G, Rao M, Rao S (2020) Prediction of wave transmission over submerged reef of tandem breakwater using PSO-SVM and PSO-ANN techniques. ISH J Hydraul Eng 26(3):283–290

Lotfy K (2019) Effect of variable thermal conductivity during the photothermal diffusion process of semiconductor medium. Silicon 11(4):1863–1873

Lu K, Zhou W, Zeng G, Zheng Y (2019) Constrained population extremal optimization-based robust load frequency control of multi-area interconnected power system. Int J Electr Power Energy Syst 105:249–271

Lu KD, Zeng GQ, Zhou W (2021) Adaptive constrained population extremal optimisation-based robust proportional-integral-derivation frequency control method for an islanded microgrid. IET Cyber-Syst Robot 3(3):210–227

Mahmood T et al (2022) Novel adaptive Bayesian regularization networks for peristaltic motion of a third-grade fluid in a planar channel. Mathematics 10(3):358

Mai S, Zille H, Steup C, Mostaghim S (2019) Multi-objective collective search and movement-based metrics in swarm robotics. In Proceedings of the genetic and evolutionary computation conference companion, pp. 387–388

Malešević N, Petrović V, Belić M, Antfolk C, Mihajlović V, Janković M (2020) Contactless real-time heartbeat detection via 24 GHz continuous-wave Doppler radar using artificial neural networks. Sensors 20(8):2351

Mehmood A et al (2020) Integrated computational intelligent paradigm for nonlinear electric circuit models using neural networks, genetic algorithms and sequential quadratic programming. Neural Comput Appl 32(14):10337–10357

Mesloub H, Benchouia MT, Boumaaraf R, Goléa A, Goléa N, Becherif M (2020) Design and implementation of DTC based on AFLC and PSO of a PMSM. Math Comput Simul 167:340–355

Nasirzadehroshenin F, Sadeghzadeh M, Khadang A, Maddah H, Ahmadi MH, Sakhaeinia H, Chen L (2020) Modeling of heat transfer performance of carbon nanotube nanofluid in a tube with fixed wall temperature by using ANN–GA. Eur Phys J Plus 135(2):1–20

Nisar K et al (2021) Design of morlet wavelet neural network for solving a class of singular pantograph nonlinear differential models. IEEE Access 9:77845–77862

Özsoy VS, Ünsal MG, Örkcü HH (2020) Use of the heuristic optimization in the parameter estimation of generalized gamma distribution: comparison of GA, DE, PSO and SA methods. Comput Stat 35(4):1895–1925

Qu N, Chen J, Zuo J, Liu J (2020) PSO–SOM neural network algorithm for series arc fault detection. Adv Math Phys. https://doi.org/10.1155/2020/6721909

Raja MAZ, Umar M, Sabir Z, Khan JA, Baleanu D (2018) A new stochastic computing paradigm for the dynamics of nonlinear singular heat conduction model of the human head. Eur Phys J Plus 133(9):364

Raja MAZ, Mehmood J, Sabir Z, Nasab AK, Manzar MA (2019) Numerical solution of doubly singular nonlinear systems using

neural networks-based integrated intelligent computing. Neural Comput Appl 31(3):793–812
Roul P, Thula K (2019) A fourth-order B-spline collocation method and its error analysis for Bratu-type and Lane-Emden problems. Int J Comput Math 96(1):85–104
Sabir Z et al (2018) Neuro-heuristics for nonlinear singular Thomas-Fermi systems. Appl Soft Comput 65:152–169
Sabir Z (2022a) Neuron analysis through the swarming procedures for the singular two-point boundary value problems arising in the theory of thermal explosion. Eur Phys J Plus 137(5):1–18
Sabir Z (2022b) Stochastic numerical investigations for nonlinear three-species food chain system. Int J Biomath 15(04):2250005
Sabir Z, Raja MAZ, Umar M, Shoaib M (2020a) Neuro-swarm intelligent computing to solve the second-order singular functional differential model. Eur Phys J Plus 135(6):1–19
Sabir Z, Amin F, Pohl D, Guirao JL (2020b) Intelligence computing approach for solving second order system of Emden-Fowler model. J Intell Fuzzy Syst 38(6):7391–7406
Sabir Z, Raja MAZ, Umar M, Shoaib M (2020c) Design of neuro-swarming-based heuristics to solve the third-order nonlinear multi-singular Emden-Fowler equation. Eur Phys J Plus 135(5):410
Sabir Z, Saoud S, Raja MAZ, Wahab HA, Arbi A (2020d) Heuristic computing technique for numerical solutions of nonlinear fourth order Emden-Fowler equation. Math Comput Simul 178:534–548
Sabir Z et al (2020e) Novel design of Morlet wavelet neural network for solving second order Lane-Emden equation. Math Comput Simul 172:1–14
Sabir Z, Umar M, Guirao JL, Shoaib M, Raja MAZ (2021a) Integrated intelligent computing paradigm for nonlinear multi-singular third-order Emden-Fowler equation. Neural Comput Appl 33(8):3417–3436
Sabir Z et al (2021b) Design of Gudermannian Neuroswarming to solve the singular Emden-Fowler nonlinear model numerically. Nonlinear Dyn 106(4):3199–3214
Sabir Z, Umar M, Raja MAZ, Baleanu D (2021c) Numerical solutions of a novel designed prevention class in the HIV nonlinear model. CMES-Comput Model Eng Sci 129(1):227–251
Sabir Z, Umar M, Raja MAZ, Baskonus HM, Gao W (2022a) Designing of Morlet wavelet as a neural network for a novel prevention category in the HIV system. Int J Biomath 15(04):2250012
Sabir Z, Umar M, Raja MAZ, Fathurrochman I, Hasan H (2022b) Design of Morlet wavelet neural network to solve the non-linear influenza disease system. Appl Math Nonlinear Sci. https://doi.org/10.2478/amns.2021.2.00120
Sabir Z, Wahab HA, Nguyen TG, Altamirano GC, Erdoğan F, Ali MR (2022c) Intelligent computing technique for solving singular multi-pantograph delay differential equation. Soft Comput 26:6701–6713
Sabir Z et al (2022d) FMNSICS: Fractional Meyer neuro-swarm intelligent computing solver for nonlinear fractional Lane-Emden systems. Neural Comput Appl 34(6):4193–4206
Sabir Z, Botmart T, Raja MAZ, Sadat R, Ali MR, Alsulami AA, Alghamdi A (2022e) Artificial neural network scheme to solve the nonlinear influenza disease model. Biomed Signal Process Control 75:103594
Saeed T et al (2022) An advanced heuristic approach for a nonlinear mathematical based medical smoking model. Results Phys 32:105137
Sharma B, Kumar S, Paswan MK, Mahato D (2019) Chebyshev operational matrix method for lane-emden problem. Nonlinear Eng 8(1):1–9
Sibalija TV (2019) Particle swarm optimisation in designing parameters of manufacturing processes: A review (2008–2018). Appl Soft Comput 84:105743
Singh R, Guleria V, Singh M (2020) Haar wavelet quasilinearization method for numerical solution of Emden-Fowler type equations. Math Comput Simul 174:123–133
Soliman MA (2019) Approximate solution for the Lane-Emden equation of the second kind in a spherical annulus. J King Saud Univ-Eng Sci 31(1):1–5
Sulaiman TA, Bulut H, Atas SS (2019) Optical solitons to the fractional Schrdinger-Hirota equation. Appl Math Nonlinear Sci 4(2):535–542
Touchent KA, Hammouch Z, Mekkaoui T (2020) A modified invariant subspace method for solving partial differential equations with non-singular kernel fractional derivatives. Appl Math Nonlinear Sci 5(2):35–48
Umar M, Amin F, Wahab HA, Baleanu D (2019) Unsupervised constrained neural network modeling of boundary value corneal model for eye surgery. Appl Soft Comput 85:105826
Umar M et al (2019) Intelligent computing for numerical treatment of nonlinear prey–predator models. Appl Soft Comput 80:506–524
Umar M, Raja MAZ, Sabir Z, Alwabli AS, Shoaib M (2020) A stochastic computational intelligent solver for numerical treatment of mosquito dispersal model in a heterogeneous environment. Eur Phys J Plus 135(7):1–23
Verma AK, Kumar N (2019) Haar wavelets collocation on a class of Emden-Fowler equation via Newton's quasilinearization and Newton-Raphson techniques. arXiv preprint arXiv:1911.05819
Verma AK, Kumar N, Singh M, Agarwal RP (2021) A note on variation iteration method with an application on Lane-Emden equations. Eng Comput 38:3932
Wambacq J, Ulloa J, Lombaert G, François S (2021) Interior-point methods for the phase-field approach to brittle and ductile fracture. Comput Methods Appl Mech Eng 375:113612
Wang B, Gomez-Aguilar JF, Sabir Z, Zahoor Raja MA, Xia WF, Jahanshahi H, Alsaadi FE (2022) Numerical computing to solve the nonlinear corneal system of eye surgery using the capability of Morlet wavelet artificial neural networks. Fractals. https://doi.org/10.1142/S0218348X22401478
Xie LJ, Zhou CL, Xu S (2019) Solving the systems of equations of Lane-Emden type by differential transform method coupled with adomian polynomials. Mathematics 7(4):377
Xie T, Liu R, Wei Z (2020) Improvement of the fast clustering algorithm improved by-means in the big data. Appl Math Nonlinear Sci 5(1):1–10
Xue Y, Sun Q, Li C, Dang W, Hao F (2021) Distribution network monitoring and management system based on intelligent recognition and judgement. Appl Math Nonlinear Sci. https://doi.org/10.2478/amns.2021.1.00057
Yang J, Wang X, Bauer P (2019) Extended PSO based collaborative searching for robotic swarms with practical constraints. IEEE Access 7:76328–76341
Yao H (2021) Application of artificial intelligence algorithm in mathematical modelling and solving. Appl Math Nonlinear Sci. https://doi.org/10.2478/amns.2021.2.00081
Yokuş A, Gülbahar S (2019) Numerical solutions with linearization techniques of the fractional Harry Dym equation. Appl Math Nonlinear Sci 4(1):35–42
Zanelli A, Domahidi A, Jerez J, Morari M (2020) FORCES NLP: an efficient implementation of interior-point methods for multistage nonlinear nonconvex programs. Int J Control 93(1):13–29
Ziane D, Cherif MH, Cattani C, Belghaba K (2019) Yang-Laplace decomposition method for nonlinear system of local fractional partial differential equations. Appl Math Nonlinear Sci 4(2):489–502